

# Effect of the Solvent on the Conformation of Isolated MEH-PPV Chains Intercalated Into SnS<sub>2</sub>

Eyal Aharon,<sup>[a]</sup> Steffen Breuer,<sup>[b]</sup> Frank Jaiser,<sup>[b]</sup> Anna Köhler,<sup>[b, c]</sup> and Gitti L. Frey\*<sup>[a]</sup>

*Photophysical processes in conjugated polymers are influenced by two competing effects: the extent of excited state delocalization along a chain, and the electronic interaction between chains. Experimentally, it is often difficult to separate the two because both are controlled by chain conformation. Here we demonstrate that it is possible to modify intra-chain delocalization without inducing inter-chain interactions by intercalating polymer monolayers between the sheets of an inorganic layered matrix. The red-emitting conjugated polymer, MEH-PPV, is confined to the interlayer space of layered SnS<sub>2</sub>. The formation of isolated polymer monolayers between the SnS<sub>2</sub> sheets is confirmed by X-ray diffraction measurements. Photoluminescence excitation (PLE) and photoluminescence (PL) spectra of the incorporated MEH-PPV chains reveal that the morphology of the incor-*

*porated chains can be varied through the choice of solvent used for chain intercalation. Incorporation from chloroform results in more extended conformations compared to intercalation from xylene. Even highly twisted conformations can be achieved when the incorporation occurs from a methanol:chloroform mixture. The PL spectra of the MEH-PPV incorporated SnS<sub>2</sub> nanocomposites using the different solvents are in good agreement with the PL spectra of the same solutions, indicating that the conformation of the polymer chains in the solutions is retained upon intercalation into the inorganic host. Therefore, intercalation of conjugated polymer chains into layered hosts enables the study of intra-chain photophysical processes as a function of chain conformation.*

## Introduction

Conjugated polymers have been the subject of extensive academic and industrial research efforts due to their promising potential for use as active layers in electronic and optoelectronic devices.<sup>[1,2]</sup> In these various applications it has been found that in addition to the intrinsic chemical properties of the polymers, the device performance is strongly dependent on the conformation of the polymer chains and the inter-chain interactions.<sup>[3-5]</sup> For example,  $\pi$ - $\pi$  interactions between neighboring chains significantly reduce intermolecular distance and affect processes such as charge transport and charge separation. Interactions between chromophores on neighboring chains can lead to the formation of excimers, exciplexes or aggregates with inefficient, unstructured red-shifted emission.<sup>[5-7]</sup> Therefore, to understand the physical processes limiting the performance of conjugated polymer devices it is necessary to isolate the polymer chains so that the inter- and intra-chain interactions are decoupled. Inter-chain interactions can be suppressed by dissolving the conjugated polymer in extremely dilute concentrations in a "good" solvent, such as xylene or chloroform,<sup>[7-9]</sup> yet, this typically results in a chain conformation that differs from that present in a solid film. To gain insight on the correlation between polymer conformation and device performance, it is therefore necessary to obtain isolation of the conjugated polymer chains in the solid state.

Several approaches have been reported for the isolation of conjugated polymer chains in the solid state, including dispersing the polymer chains at extremely dilute concentrations in an insulating polymer matrix such as PMMA, polystyrene or polyethylene,<sup>[10-12]</sup> threading the polymer chains through cy-

clodextrins,<sup>[13]</sup> or shearing the polymer chains between mica plates.<sup>[14]</sup> Mechanical shearing of polymer powders can insert defects into the polymer chains transforming them into entirely different, non-conjugated species. Isolating conjugated macromolecules in polyrotaxane architectures has been demonstrated for judiciously designed short conjugated oligomers, but will not be efficient to fully suppress interchain interactions in commercially available, high molecular weight conjugated polymers.<sup>[13,15]</sup> Dispersing dilute commercial conjugated polymer chains in insulating polymer matrices, on the other hand, is simple, but requires sophisticated measurements and expensive experimental tools to detect the resulting low optical signals. Furthermore, the dispersed chains attain a wide and uncontrollable distribution of chain morphologies and conformations obscuring the desired structure-property correlation. Therefore, to study the intra-molecular photophysical processes occurring in isolated conjugated polymer chains as a function of chain conformation, it is necessary to isolate a large

[a] E. Aharon, Dr. G. L. Frey  
Department of Materials Engineering  
Technion-Israel Institute of Technology  
Haifa 32000 (Israel)  
Fax: (+972) 4-8295677  
E-mail: gitti@tx.technion.ac.il

[b] S. Breuer, Dr. F. Jaiser, Prof. A. Köhler  
Department of Physics, University of Potsdam  
Potsdam 14469 (Germany)

[c] Prof. A. Köhler  
Department of Physics, University of Bayreuth  
Potsdam 95440 (Germany)

number of polymer chains all attaining the same chain conformation.

Conformational control of a large population of isolated chains can be achieved by geometrically restricting the polymer chains into spatially well-defined voids of 3D or 2D porous matrices.<sup>[16,17]</sup> In the latter, the conjugated polymers are incorporated into the inter-layer galleries of a layered compound. The 2D layered host materials, such as clays, layered metal oxides and layered metal chalcogenides, have sheet-like structures that are characterized by strong covalent bonds within the layers and weak van der Waals forces between the layers. Consequently, the interlayer space can be considerably separated to incorporate guest polymers while preserving the integrity of the layer structure.<sup>[18]</sup> Several methodologies have been developed for the incorporation of polymer chains into the interlayer galleries of layered compounds including polymer infiltration,<sup>[19]</sup> in-situ polymerization,<sup>[20]</sup> and exfoliation-adsorption. In the latter, the host stacks are delaminated into single layers, followed by their flocculation in the presence of the guest polymeric species, effectively encapsulating the polymer chains in between adjacent layers.<sup>[21]</sup>

Recently, a blue-emitting polymer, PFO (poly 9,9-dioctylfluorene), was incorporated into the interlayer-space of layered silicates<sup>[16]</sup> and layered sulfides.<sup>[22]</sup> In both cases, confining the polymer chains within the spatially-limited planar gallery prevented the  $\pi$ -stacking of polymer chains. Decoupling of the inter- and intra-chain interactions provided control over the optoelectronic processes in the composites and corresponding devices. Intercalation of PFO and MEH-PPV into layered silicates improved its color purity and the luminescence stability, and corresponding light emitting diodes (LEDs) showed an enhancement of exciton recombination and electroluminescence efficiency compared to pristine polymer devices.<sup>[16,23,24]</sup> Co-intercalation of blue, green and red emitting polymers into semiconducting<sup>[25]</sup> layered  $\text{SnS}_2$  resulted in simultaneous emission from the three polymers, that is, white emission.<sup>[26]</sup> The white photo- and electro-luminescence, an elusive challenge for organic light emitting diodes, was obtained due to the suppression of the efficient energy transfer between co-facially stacked polymer chains when incorporated into the layered host.

Herein, we demonstrate that intercalation into layered hosts can also provide control over the conformation of the incorporated isolated conjugated polymer chains by judicious selection of the solvent used for the polymer intercalation. In this study, the red-emitting polymer, MEH-PPV [poly (2-methoxy-5-(2'-ethyl-hexyloxy)-1,4-phenylene vinylene)], is intercalated into  $\text{SnS}_2$  from a variety of solvents and solvent mixtures. Photoluminescence excitation and photoluminescence spectra of the incorporated polymer chains show that the conformation of the polymer chain in solution is retained upon intercalation into the inorganic host. More specifically, MEH-PPV chains intercalated into  $\text{SnS}_2$  from chloroform showed more planar conformation, compared to those intercalated from *o*-xylene or a methanol:chloroform mixture. Therefore, the conjugated polymer/layered compound guest/host nanocomposites provide a platform to study conformation-dependant photophysical processes in conjugated polymer chains that contribute insights

to the design of organic optoelectronic devices with enhanced performances.

## Results and Discussion

The optical absorption and emission spectra of conjugated polymer films depend on a variety of controllable parameters including: the polymer molecular weight,<sup>[28]</sup> the deposition technique<sup>[29,30]</sup> and parameters<sup>[31]</sup>, the nature of solvent used to prepare the solutions from which the film is cast,<sup>[9,32,33]</sup> and the concentration of the polymer in the solution.<sup>[3,34]</sup> The conformation of MEH-PPV chains in dilute solutions depend on the interactions between the polymer chains and the solvent molecules. MEH-PPV dissolves in both aromatic and non-aromatic solvents such as xylene/toluene and chloroform, respectively,<sup>[32]</sup> but the conformation of the dissolved chains depends on the solvent. In toluene, for example, MEH-PPV chains tend to minimize interactions with the solvent by backbone twists, while in chloroform the polymer backbone has an extended conformation.<sup>[8,9]</sup> Consequently, the absorption and emission spectra of dilute MEH-PPV solutions in xylene are weighted to the blue compared to those with the same concentration but in chloroform, as shown in Figure 1. MEH-PPV solutions in chloroform

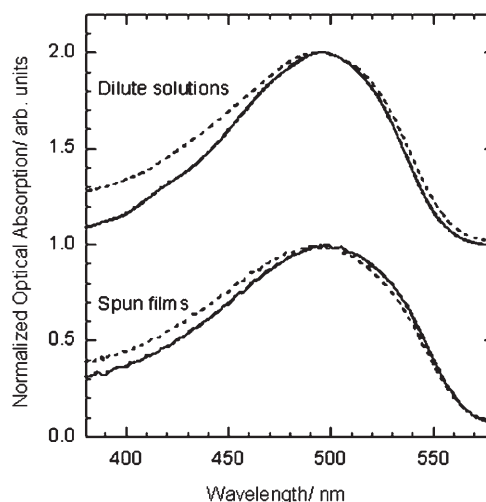


**Figure 1.** Room-temperature optical absorption spectra of MEH-PPV dilute solutions,  $0.01 \text{ mg mL}^{-1}$ , and corresponding spun films in chloroform (—) or *o*-xylene (----).

and *o*-xylene both show a broad absorption peak centered at 495 nm, associated with the fundamental  $\pi$ - $\pi^*$  transition, but the *o*-xylene solution also shows significant contributions of high-energy transitions in the wavelength range below 500 nm. These transitions originate from the twisted, shortly conjugated MEH-PPV segments in *o*-xylene that are not present in the chloroform solution.

The conformations of the MEH-PPV chains in solution are partially preserved in the corresponding spun films, as evident from the differences between the absorption spectra of films spun from chloroform and *o*-xylene in the high energy (< 500 nm) region (Figure 1). However, these differences are

smaller than those observed for the solutions because solvent evaporation during film forming induces conformation changes and interchain interactions leading to more extended conformations.<sup>[33,35]</sup> Therefore, to study the conformation-dependent optical properties of isolated MEH-PPV in the solid state, it is necessary to inhibit inter-chain interaction during film processing. These conditions are achieved by intercalating MEH-PPV into sterically restricted galleries of layered matrices. The spatial confinement in the planar galleries hinders polymer aggregation and  $\pi$ - $\pi$  inter-chain interactions,<sup>[26]</sup> and was recently shown to reduce excitation transfer compared to that in a pristine polymer film.<sup>[36]</sup>

Incorporation of conjugated polymers into layered  $\text{SnS}_2$ , a wide-gap semiconductor transparent to MEH-PPV emission,<sup>[37]</sup> was recently reported using the exfoliation-restack method.<sup>[26]</sup> In this process, Li atoms are intercalated into the inter-layer galleries of  $\text{SnS}_2$ , followed by  $\text{Li}_x\text{SnS}_2$  exfoliation to form a suspension of  $\text{SnS}_2$  single layers. Restacking the  $\text{SnS}_2$  layers in the presence of MEH-PPV effectively encapsulates the polymer chains between two adjacent  $\text{SnS}_2$  layers. Herein, MEH-PPV and exfoliated  $\text{SnS}_2$  are co-assembled in three different solutions to examine the influence of the solvent on the conformation of the incorporated polymer chains. The selected solvents were chloroform, *o*-xylene and a mixture of chloroform and methanol (1:1 vol%), each known to influence the MEH-PPV conformation in solution. Chloroform and xylene induce extended and less extended conformations of MEH-PPV chains, respectively.<sup>[8,38,39]</sup> Addition of methanol, a poor solvent for MEH-PPV, to a chloroform MEH-PPV solution, decreases the chains effective conjugation length and solubility, leading to a collapsed coiled conformation.<sup>[9,40,41]</sup> The restacked nanocomposite powders are subsequently washed in the same solvent used for the nanocomposite restack to remove non-incorporated MEH-PPV, and cast into thin films (see Experimental Section). A schematic illustration of the exfoliation-restack process, along with the chemical structure of MEH-PPV, is shown in Figure 2a.

X-ray measurements of the restacked films, Figure 2, confirm that MEH-PPV is successfully intercalated into the interlayer galleries of  $\text{SnS}_2$ , regardless of the solvent used for the intercalation. The patterns of as-received  $\text{SnS}_2$  powder, and  $\text{SnS}_2$  restacked without polymer in Figure 2b show an intense reflection at  $5.8 \text{ \AA}$  ( $2\theta = 15.4^\circ$ ), corresponding to the *c*-axis interlayer spacing of  $\text{SnS}_2$  single crystals.<sup>[18]</sup> The reflection broadening after exfoliation and restack indicates a reduction in the number of layers in a  $\text{SnS}_2$  stack. A very broad weak reflection in the vicinity of  $\sim 9 \text{ \AA}$  ( $2\theta = 10^\circ$ – $11^\circ$ ) is observed in the pattern of the  $\text{SnS}_2$  restacked with no polymer, assigned to the intercalation of methanol molecules between the restacked  $\text{SnS}_2$  sheets.<sup>[42]</sup>

The patterns of  $\text{SnS}_2$  restacked with MEH-PPV in chloroform or *o*-xylene in Figure 2b, show two additional strong new peaks at  $\sim 11 \text{ \AA}$  ( $2\theta \sim 8^\circ$ ), and  $\sim 5.5 \text{ \AA}$  ( $2\theta \sim 16^\circ$ ), assigned to the (001) and (002) reflections of MEH-PPV-incorporated  $\text{SnS}_2$ . These reflections are also noticeable, although weakly, in the pattern of the film restacked with MEH-PPV from a 1:1 vol% chloroform:methanol mixture. The expansion of the interlayer spacings by  $\sim 5 \text{ \AA}$ , to accommodate the MEH-PPV guest spe-

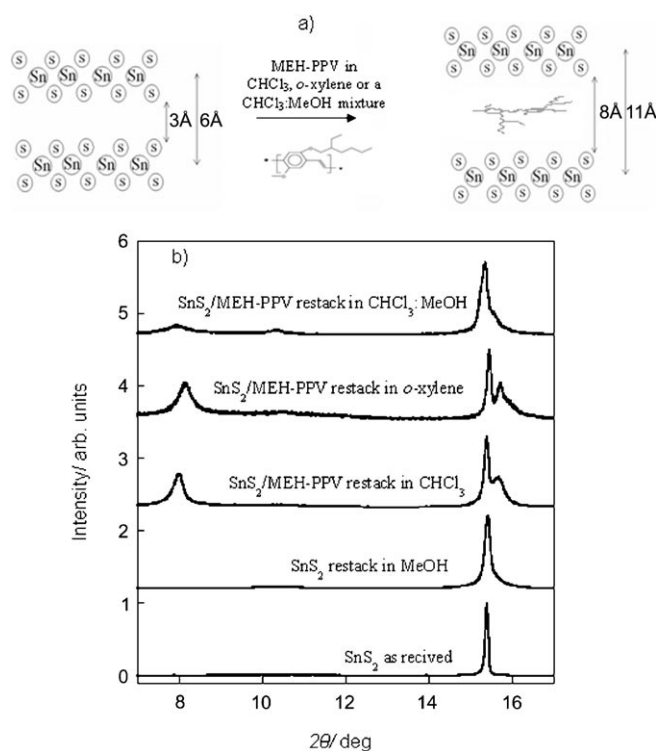


**Figure 2.** a) Schematic illustration of MEH-PPV intercalation into the van der Waals gap of  $\text{SnS}_2$ , b) XRD patterns of as-received  $\text{SnS}_2$  powders and  $\text{SnS}_2$  exfoliated and restacked without or with MEH-PPV in different solvents.

cies, is in good agreement with the *c*-axis expansion observed for the intercalation of PANI<sup>[43]</sup> and polyfluorenes<sup>[22]</sup> monolayers into layered hosts. Figure 2a shows a schematic illustration of a MEH-PPV chain, in its stretched conformation, occupying  $3.65 \text{ \AA}$ ,<sup>[44]</sup> with some free torsion along the polymer backbone, incorporated between adjacent  $\text{SnS}_2$  layers. The scanning electron microscopy (SEM) image of the  $\text{SnS}_2$  thin film restacked with MEH-PPV from chloroform, Figure 3, shows  $\text{SnS}_2$  platelets with the *c*-axis aligned mainly perpendicular to the substrate. This film morphology is typical of all exfoliated and restacked

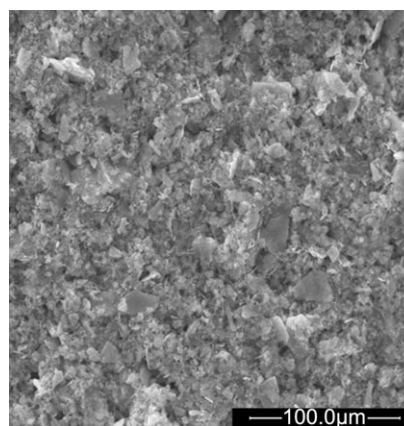


**Figure 3.** SEM image of a  $\text{SnS}_2$  thin film restacked with MEH-PPV from chloroform.

SnS<sub>2</sub> thin films used in this study, with or without polymer intercalation.

The broad intercalation reflections in the X-ray patterns of the MEH-PPV-incorporated SnS<sub>2</sub> nanocomposites obscure the correlation of the interlayer expansion with the conformation of the incorporated chains. Similarly, scattering of light by the inorganic host platelets precludes absorption spectra to be taken. Therefore, the conformation of the intercalated MEH-PPV chains was analyzed by photoluminescence excitation spectroscopy (PLE). The PLE spectra were constructed by measuring the photoluminescence spectrum as a function of excitation wavelength, and plotting the area under the emission peak as a function of excitation wavelength. This procedure ensures that the PLE spectra correspond directly to the optical absorption spectra. To allow for direct correlation of the PLE spectra with the absorption spectra, PLE spectra were taken from both nanocomposites and pristine MEH-PPV films, and are presented in Figure 4. The PLE experiments were per-

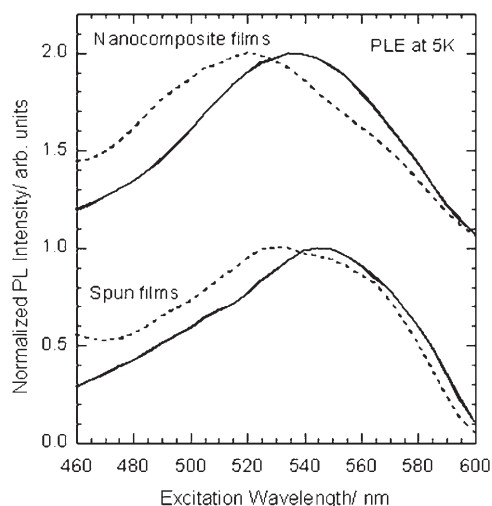


**Figure 4.** PLE spectrum (measured at 5 K) of MEH-PPV spun films and MEH-PPV incorporated into SnS<sub>2</sub>. The polymer solvents used are chloroform (—) or xylene (----).

formed at 5 K to substantially improve the signal-to-noise ratio of the spectra. The absorption of MEH-PPV is well-known to significantly shift to the red, and shows better resolved peaks at reduced temperatures. For example, the room temperature broad absorption band centered at about 500 nm (Figure 1), shifts to 530 nm and a shoulder appears at 550 nm when the temperature is reduced to 23 K.<sup>[45]</sup>

The PLE spectra taken from pristine MEH-PPV films, shown in Figure 4 (bottom panel), closely resemble the reported low temperature absorption spectra of MEH-PPV films.<sup>[45]</sup> The 5 K PLE spectrum of the film spun from xylene is red shifted compared to its room temperature absorption spectrum, and exhibits shoulders around 565 and 530 nm. The 5 K PLE spectrum of the film spun from chloroform shows a broad peak centered at 550 nm, which is also red shifted compared to its room temperature absorption spectrum, but does not show additional

high-energy contributions. The differences between the PLE spectra of the pristine films deposited from xylene or chloroform reflect the different distribution of conjugation lengths present in both films. In the case of the pristine films deposited from xylene, the short conjugated chain conformation of the polymer chains in solution is partially retained in the films, and hence, the PLE spectrum shows intense contributions in the high-energy region. These high-energy transitions are less abundant in the films deposited from chloroform due to the more extended conformation of the chains in chloroform solutions. Therefore, the PLE spectra of the pristine films presented in Figure 4 are in good agreement with the absorption spectra shown in Figure 1, and corroborate that films deposited from chloroform include mainly extended conformations, while those deposited from xylene include a high population of short-conjugated segments retaining their solution conformation, and also extended conformations which were either present in the solution or induced during film processing.

The type of solvent used for preparing the nanocomposites, xylene or chloroform, also has a strong effect on the PLE spectra, as shown in Figure 4 (top panel). However, while the type of solvent used for the deposition of pristine films affects the high-energy range (<530 nm) of the PLE spectrum, (Figure 4, bottom panel); the PLE spectra of the nanocomposites prepared from xylene or chloroform also differ significantly in the low-energy region (>530 nm) (Figure 4, top panel). As for the pristine films, the intense contributions in the high-energy part of the xylene-prepared nanocomposite PLE spectrum are attributed to the presence of MEH-PPV chains preserving their xylene solution short-conjugated conformations upon intercalation into SnS<sub>2</sub>. These conformations are scarce in chloroform solutions and are thus absent in the chloroform-prepared nanocomposites.

The preservation of the xylene or chloroform solution conformations upon intercalation into the layered host from the corresponding solutions is even more pronounced in the low-energy region of the nanocomposites PLE spectra. In pristine films, low-energy PLE spectra of xylene and chloroform are comparable, representing a similar population of extended conformations in both films. In contrast in the nanocomposites, the intensity of the low-energy PLE signal is substantially lower for samples prepared from xylene than for chloroform-prepared nanocomposites. This suggests the nanocomposites prepared from xylene contain only few chains with extended conformations, in contrast to the situation in the pristine film. In the xylene-deposited pristine film, extended conformations can be induced by interchain interactions during solvent evaporation and film deposition.<sup>[3,35]</sup> During MEH-PPV incorporation into SnS<sub>2</sub>, on the other hand, the spatial limitations imposed by the  $\approx 10$  Å interlayer spacing of the host suppress interchain interactions, and hence sample processing does not induce extended conformations. Consequently, the distribution of MEH-PPV chain conformations in the solutions, xylene or chloroform, are preserved upon intercalation into the layered SnS<sub>2</sub> matrix. In particular, they are not modified by interchain interactions during film preparation. We conclude, therefore, that judicious selection of the solvent used for the polymer in-

tercalation can provide control over the conformation of the incorporated conjugated polymer chains.

The reduced interchain interactions during nanocomposite preparation and film deposition, compared to those present during pristine film deposition, are also evident by comparing the PLE spectra of the pristine films (Figure 4, lower panel) with those obtained from nanocomposite films prepared using the same solvents (Figure 4, upper panel). In general, the intensity in the low-energy region (for wavelengths longer than 550 nm) is reduced in the nanocomposite spectra compared to the respective pristine film, leading to an overall apparent ~10 nm blue shift of the nanocomposite PLE spectra. This blue shift is associated with the fact that, in contrast to pristine films, nanocomposite processing does not induce extended morphologies during solvent evaporation and film deposition. Therefore, the low-energy transitions in the PLE spectra of the nanocomposites are much weaker than those in the PLE spectra of the corresponding pristine films.

The preservation of MEH-PPV solution conformations upon incorporation into SnS<sub>2</sub> is also demonstrated in the photoluminescence spectra of the nanocomposites. The photoluminescence (PL) spectra of pristine polymer and nanocomposite films prepared from chloroform, *o*-xylene and a 1:1 (vol) chloroform:methanol mixture, are shown in Figure 5. We shall first focus on the PL spectra of pristine and nanocomposite films deposited from xylene or chloroform solutions, and then turn to the PL of nanocomposites prepared from the solvent mixture containing methanol.

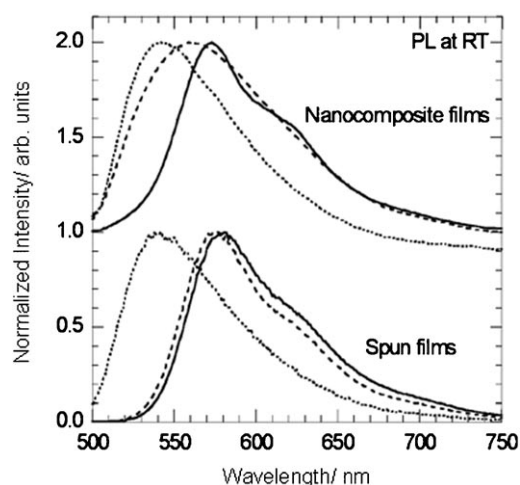


**Figure 5.** RT photoluminescence spectra (excited at 420 nm) of pristine MEH-PPV spun films and MEH-PPV-incorporated SnS<sub>2</sub>. The polymer solvents used are chloroform (—), *o*-xylene (---), or a 1:1 vol% chloroform:methanol mixture (.....).

The PL spectrum of the pristine films deposited from chloroform and *o*-xylene are similar to each other with the transitions at ~580 and 620 nm, associated with the 0–0 and 0–1 vibronic transitions, respectively.<sup>[3]</sup> Photoluminescence of conjugated polymers in the solid state originates mainly from the highly extended segments (lowest gap chromophores) due to extremely efficient energy transfer.<sup>[34,46]</sup> The similar spectra we

obtain for films spun from chloroform and xylene thus suggests that both films contain planarised segments, with the slight red shift of the chloroform deposited spectrum suggesting more extended conformations in the chloroform film compared to the *o*-xylene deposited film.

The conformations of the MEH-PPV chains incorporated into SnS<sub>2</sub> from *o*-xylene are distinctly different from those incorporated from chloroform, as evident from the considerably broader and blue-shifted (~15 nm) PL spectrum of the nanocomposites prepared from *o*-xylene compared to that of nanocomposites prepared from chloroform. Moreover, the PL spectrum of the chloroform prepared nanocomposites shows well-resolved vibronic features with the 0–0 and 0–1 vibronic transitions centered at ~572 and 617 nm, respectively. The PL spectrum of the nanocomposites prepared from *o*-xylene, on the other hand, is a broad featureless peak centered at ~562 nm.

As mentioned above, photoluminescence spectra give a signature of the spectral diffusion of the excited state that exists in the density of states provided by the different conformers in a polymer film. Dimensionality of conjugated polymer systems plays an important role in this energy transfer process, with one-dimensional intra-chain transfer of excitations typically being much slower than that between  $\pi$ -stacked chains within a three-dimensional polymeric solid.<sup>[17,47]</sup> Recently, it was shown that energy transfer in the quasi-two-dimensional polymer monolayers incorporated into layered matrices is substantially suppressed compared to that in a three-dimensional polymeric solid.<sup>[36]</sup> Therefore, in contrast to the PL spectra of pristine films, the PL spectra of MEH-PPV chains incorporated into the layered host are not entirely dominated by the highly extended conformations, but rather represent a broader distribution of conjugation lengths and chain conformations.

The suppressed energy transfer in the nanocomposites suggests that the dramatic differences between the PL spectra of the nanocomposites prepared from *o*-xylene and chloroform, originate from the differences in the conformations of the MEH-PPV chains incorporated from the two distinct solvents. More specifically, intercalation from *o*-xylene leads to a broad distribution of MEH-PPV chain-conformations with a large population of short conjugation segments, evident from the broad featureless peak with intense transitions in the high-energy region (<550 nm). In contrast, MEH-PPV chains incorporated from chloroform exhibit a narrow distribution of extended conformations; evident from the vibronic features of the PL spectrum and its resemblance to that of the corresponding pristine film. Therefore, the PL spectra corroborate that the conformations of MEH-PPV chains in solution are maintained during the intercalation process into SnS<sub>2</sub>.

Intercalation of conjugated polymer chains into a layered matrix can provide a platform to study the correlation between chain morphology and the optical properties in the solid state, because the conformation of the chains is controlled by the solvent used, and energy transfer between the chains is geometrically suppressed. In order to demonstrate that even extreme conformations can be preserved by this technique, MEH-PPV chains were intercalated into SnS<sub>2</sub> from a chloroform:methanol mixture (1:1 vol). The mixture was filtered in order to

extract large aggregates induced by interchain interactions, and maintain only isolated chains in the solution (see Experimental Section). Methanol, a poor solvent for MEH-PPV, induces a collapse coiled conformation of the polymer chains and dramatically reduces the conjugation length of the chains in solution. Accordingly, the PL spectrum of a pristine film prepared from the chloroform:methanol mixture is substantially blue shifted ( $>30$  nm) compared to that of a film prepared from chloroform only, as shown in Figure 5. The PL spectrum of the MEH-PPV film deposited from the chloroform:methanol mixture is similar to that of the MEH-PPV chains isolated in PMMA, because interchain interactions during the rapid co-evaporation of the methanol (b.p.  $64.7^{\circ}\text{C}$ ) and chloroform (b.p.  $61.2^{\circ}\text{C}$ ) are not sufficient to induce extension of the conjugation lengths.

The highly coiled conformation of the MEH-PPV chains in the chloroform:methanol mixture are preserved upon intercalation into  $\text{SnS}_2$  as evident from their PL spectra presented in Figure 5. The PL spectrum of the nanocomposites prepared from the chloroform:methanol mixture is broad and featureless reflecting a wide distribution of conjugation lengths in the incorporated MEH-PPV chains. Moreover, the spectrum is 22 and 32 nm blue-shifted, compared to that of MEH-PPV chains intercalated into  $\text{SnS}_2$  from *o*-xylene or pure chloroform. The significant effect of the solvent type on the PL spectra of MEH-PPV chains incorporated into  $\text{SnS}_2$  demonstrates that incorporation of conjugated polymer chains into layered hosts provides control over the confirmation of a large number of polymer chains in the solid state, in contrast with pristine films where the solvent evaporation induces unavoidable and uncontrollable aggregation and extension of the polymer chains.

## Conclusions

In this study the red-emitting conjugated polymer, MEH-PPV, was confined to the interlayer space of a semiconducting inorganic layered matrix,  $\text{SnS}_2$ , from a variety of solvents and solvent mixtures. X-ray diffraction measurements indicate that regardless of the solvent used, a single conjugated polymer monolayer is isolated between the inorganic sheets, so that polymer aggregation or  $\pi$ - $\pi$  interchain interactions are significantly reduced. The photoluminescence excitation (PLE) and photoluminescence (PL) spectra of the incorporated MEH-PPV chains indicate that the conformation of the polymer chains in solution is retained upon intercalation into the inorganic host. Therefore, the conjugated polymer/layered compound guest/host nanocomposites provide a simple platform to study conformation-dependent photophysical processes in conjugated polymer chains that could contribute insights to the design of organic optoelectronic devices with enhanced performances.

## Experimental Section

**Materials:** Poly[2-methoxy-5-(2'-ethyl-hexyloxy)-1,4-phenylene vinylene] (MEH-PPV,  $M_w = 500$  kDa, American Dye Source inc., Quebec, Canada),  $\text{SnS}_2$  powder (Alfa Aesar), *n*-butyllithium (1.6 M in hexane, Aldrich), hexane (95% anhydrous, Aldrich), methanol

(99.9%, SPECTRO-PH, Aldrich), *o*-xylene (98%, HPLC grade, Aldrich) and chloroform (Bio-Lab Ltd) were used as received.

**Nanocomposite Synthesis and Film Deposition:** MEH-PPV was dissolved ( $1\text{ mg mL}^{-1}$ ) separately in *o*-xylene or chloroform. The solutions were stirred on a hot plate ( $60^{\circ}\text{C}$ ) for five hours and then filtered through a  $0.45\ \mu\text{m}$  filter. To obtain a homogenous solution of MEH-PPV in a methanol:chloroform 1:1 vol% mixture, a  $0.5\text{ mg mL}^{-1}$  solution was prepared and sonicated for two hours. Then, the solution was filtered through a  $0.45\ \mu\text{m}$  filter in order to eliminate the aggregations and maintain only the isolated coiled chains in the solution.

Incorporation of MEH-PPV into  $\text{SnS}_2$  was achieved by the intercalation and exfoliation method.  $\text{Li}_x\text{SnS}_2$  was prepared by soaking  $\text{SnS}_2$  powder in BuLi in hexane, at Sn/Li molar ratio of 1:5, for five days under nitrogen atmosphere, following the procedure reported by Murphy et al.<sup>[27]</sup> After five days the solvent was extracted and the powder was dried under nitrogen for 24 h. Typically, 40 mg of the dry  $\text{Li}_x\text{SnS}_2$  were exfoliated in 2 mL methanol under sonication in ambient conditions for two hours. The  $\text{SnS}_2$  suspension was then separately mixed with 8 mL of the MEH-PPV solutions (in either chloroform, *o*-xylene or methanol:chloroform 1:1 vol% mixture), and stirred for one week. The  $\text{SnS}_2$ /MEH-PPV nanocomposite suspensions were then centrifuged and washed, each in the respective solvent used for the MEH-PPV solution, until no trace of MEH-PPV was found in the absorption spectra of the supernatant solution. The sediment was then re-suspended in 4 mL of the respective MEH-PPV solvent and cast into thin films.

For comparison, pristine MEH-PPV thin films were spun (1500 rpm, 60 sec) from the same *o*-xylene, chloroform and methanol:chloroform solutions for photoluminescence measurements, and from *p*-xylene or chloroform for photoluminescence excitation measurements. Five samples of each sample type, pristine spun films and nanocomposite films, were measured and the variation of PL peak position was 2–3 nm for all sets of samples.

**Characterization:** X-ray diffraction (XRD) measurements were performed on a Philips X-Pert diffractometer using a  $\text{Cu}_{K\alpha}$  X-ray source at wavelength  $1.54\ \text{\AA}$ .

Scanning electron microscopy (SEM) measurements were carried out using a Quanta 200 FEI-USA tungsten filament gun Environmental SEM at accelerating voltage of 25 kV.

Optical absorption and photoluminescence (PL) measurements at room temperature were performed on a Cary 100 spectrophotometer and Cary Eclipse spectrofluorometer, respectively. For the PL measurements, the excitation wavelength was 420 nm with excitation and emission filters that have optical windows at 300–500 nm and above 515 nm, respectively. Horizontal and vertical polarizers were placed between the source and sample, and the sample and detector, respectively, to remove stray light.

Photoluminescence Excitation (PLE) measurements were performed using a frequency tripled Nd:YAG laser (Spectron) and an optical parametric oscillator system (GWU VisIR 2/120) as a tunable excitation wavelength. The photoluminescence spectra were recorded with an Andor iDus CCD coupled to a LOT-Oriel MSH-201 monochromator. During the measurement, the sample was kept at 5 K in an Oxford instruments OptistatCF Cryostat. A longpass filter with an absorption edge at 650 nm was used to exclude stray light from the excitation. The excitation wavelength was chosen from 450 nm to 610 nm in steps of 5 nm. For each step, the laser intensity was measured using a thermal laser power meter in order to normalize the recorded PL spectrum. The PLE spectrum was finally constructed by plotting the integrated PL intensity as a function of excitation wavelength.

## Acknowledgements

This project was funded by the German–Israeli Foundation for Scientific Research & Development (GIF), contract number I-897-221.10/2005, and the Minerva Stiftung Short-Term Research Grant.

**Keywords:** conjugated polymers · intercalation · nanocomposites · photoluminescence · photophysics

- [1] J. H. Burroughes, D. D. C. Bradley, A. R. Brown, R. N. Marks, K. Mackay, R. H. Friend, P. L. Burns, A. B. Holmes, *Nature* **1990**, *347*, 539–541.
- [2] S. Gunes, H. Neugebauer, N. S. Sariciftci, *Chem. Rev.* **2007**, *107*, 1324–1338.
- [3] T. Q. Nguyen, I. B. Martini, J. Liu, B. J. Schwartz, *J. Phys. Chem. B* **2000**, *104*, 237–255.
- [4] J. Cornil, D. Beljonne, J. P. Calbert, J. L. Bredas, *Adv. Mater.* **2001**, *13*, 1053–1067.
- [5] J. Cornil, D. A. dos Santos, X. Crispin, R. Silbey, J. L. Bredas, *J. Am. Chem. Soc.* **1998**, *120*, 1289–1299.
- [6] A. Köhler, J. S. Wilson, R. H. Friend, *Adv. Mater.* **2002**, *14*, 701–707.
- [7] T. Q. Nguyen, B. J. Schwartz, *J. Chem. Phys.* **2002**, *116*, 8198–8208.
- [8] T. Huser, M. Yan, L. J. Rothberg, *Proc. Natl. Acad. Sci. USA* **2000**, *97*, 11187–11191.
- [9] R. Traiphol, P. Sanguansat, T. Srikihirin, T. Kerdcharoen, T. Osotchan, *Macromolecules* **2006**, *39*, 1165–1172.
- [10] Z. H. Yu, P. F. Barbara, *J. Phys. Chem. B* **2004**, *108*, 11321–11326.
- [11] G. F. He, Y. F. Li, J. Liu, Y. Yang, *Appl. Phys. Lett.* **2002**, *80*, 4247–4249.
- [12] L. Smilowitz, A. Hays, A. J. Heeger, G. Wang, J. E. Bowers, *J. Chem. Phys.* **1993**, *98*, 6504–6509.
- [13] F. Cacialli, J. S. Wilson, J. J. Michels, C. Daniel, C. Silva, R. H. Friend, N. Severin, P. Samori, J. P. Rabe, M. J. O'Connell, P. N. Taylor, H. L. Anderson, *Nat. Mater.* **2002**, *1*, 160–164.
- [14] S. C. Bae, Z. Q. Lin, S. Granick, *Macromolecules* **2005**, *38*, 9275–9279.
- [15] V. Balzani, A. Credi, F. M. Raymo, J. F. Stoddart, *Angew. Chem.* **2000**, *112*, 3484–3530; *Angew. Chem. Int. Ed.* **2000**, *39*, 3348–3391.
- [16] J. H. Park, Y. T. Lim, O. O. Park, J. K. Kim, J. W. Yu, Y. C. Kim, *Adv. Funct. Mater.* **2004**, *14*, 377–382.
- [17] T. Q. Nguyen, J. Wu, S. H. Tolbert, B. J. Schwartz, *Adv. Mater.* **2001**, *13*, 609–611.
- [18] J. Morales, J. Santos, J. R. R. Barrado, J. P. Espinos, A. R. Gonzalez-Elipe, *J. Solid State Chem.* **2000**, *150*, 391–398.
- [19] R. A. Vaia, H. Ishii, E. P. Giannelis, *Chem. Mater.* **1993**, *5*, 694–1696.
- [20] M. G. Kanatzidis, C. G. Wu, H. O. Marcy, C. R. Kannewurf, *J. Am. Chem. Soc.* **1989**, *111*, 4139–4141.
- [21] W. M. R. Divigalpitiya, R. F. Frindt, S. R. Morrison, *Science* **1989**, *246*, 369–371.
- [22] E. Aharon, A. Albo, M. Kalina, G. L. Frey, *Adv. Funct. Mater.* **2006**, *16*, 980–986.
- [23] T. W. Lee, O. O. Park, J. M. Hong, D. Y. Kim, Y. C. Kim, *Thin Solid Films* **2001**, *393*, 347–351.
- [24] T. W. Lee, O. O. Park, J. H. Yoon, J. J. Kim, *Adv. Mater.* **2001**, *13*, 211–213.
- [25] G. Domingo, R. S. Itoga, Cr. Kannewurf, *Phys. Rev.* **1966**, *143*, 536–541.
- [26] E. Aharon, M. Kalina, G. L. Frey, *J. Am. Chem. Soc.* **2006**, *128*, 15968–15969.
- [27] D. W. Murphy, F. J. Disalvo, G. W. Hull, J. V. Waszczak, *Inorg. Chem.* **1976**, *15*, 17–21.
- [28] S. Shaked, S. Tal, Y. Roichman, A. Razin, S. Xiao, Y. Eichen, N. Tessler, *Adv. Mater.* **2003**, *15*, 913–916.
- [29] Y.-F. Huang, A. R. Inigo, C.-C. Chang, K.-C. Li, C.-F. Liang, C.-W. Chang, T.-S. Lim, S.-H. Chen, J. D. White, U.-S. Jeng, A.-C. Su, Y.-S. Huang, K.-Y. Peng, S.-A. Chen, W.-W. Pai, C.-H. Lin, A. R. Tameev, S. V. Novikov, A. V. Vannikov, W.-S. Fann, *Adv. Funct. Mater.* **2007**, *17*, 2902–2910.
- [30] S. A. Amautov, E. M. Nechvolodova, A. A. Bakulin, S. G. Elizarov, A. Khodarev, D. S. Martyanov, D. Y. Paraschuk, *Synth. Met.* **2004**, *147*, 287–291.
- [31] Y. Shi, J. Liu, Y. Yang, *J. Appl. Phys.* **2000**, *87*, 4254–4263.
- [32] R. Traiphol, N. Charoenthai, T. Srikihirin, T. Kerdeharoen, T. Osotchan, T. Maturros, *Polymer* **2007**, *48*, 813–826.
- [33] B. J. Schwartz, *Annu. Rev. Phys. Chem.* **2003**, *54*, 141–172.
- [34] O. Mirzov, I. G. Scheblykin, *Phys. Chem. Chem. Phys.* **2006**, *8*, 5569–5576.
- [35] T. Q. Nguyen, V. Doan, B. J. Schwartz, *J. Chem. Phys.* **1999**, *110*, 4068–4078.
- [36] P. Parkinson, E. Aharon, M. H. Chang, C. Dosche, G. L. Frey, A. Kohler, L. M. Herz, *Phys. Rev. B* **2007**, *75*, 165206–165206.
- [37] L. Amalraj, C. Sanjeeviraja, M. Jayachandran, *J. Cryst. Growth* **2002**, *234*, 683–689.
- [38] C. L. Gettinger, A. J. Heeger, J. M. Drake, D. J. Pine, *J. Chem. Phys.* **1994**, *101*, 1673–1678.
- [39] I. D. W. Samuel, B. Crystall, G. Rumbles, P. L. Burn, A. B. Holmes, R. H. Friend, *Chem. Phys. Lett.* **1993**, *213*, 472–478.
- [40] H. R. Zhang, X. F. Lu, Y. Li, X. C. Ai, X. K. Zhang, G. Q. Yang, *J. Photochem. Photobiol. A* **2002**, *147*, 15–23.
- [41] G. Padmanaban, S. Ramakrishnan, *J. Phys. Chem. B* **2004**, *108*, 14933–14941.
- [42] S. Nakagaki, A. S. Mangrich, F. Wypych, *Inorg. Chim. Acta* **1997**, *254*, 213–217.
- [43] M. G. Kanatzidis, R. Bissessur, D. C. Degroot, J. L. Schindler, C. R. Kannewurf, *Chem. Mater.* **1993**, *5*, 595–596.
- [44] C. Y. Yang, F. Hide, M. A. Diaz-Garcia, A. J. Heeger, Y. Cao, *Polymer* **1998**, *39*, 2299–2304.
- [45] M. G. Harrison, J. Gruner, G. C. W. Spencer, *Phys. Rev. B* **1997**, *55*, 7831–7849.
- [46] H. Bassler, B. Schweitzer, *Acc. Chem. Res.* **1999**, *32*, 173–182.
- [47] D. Beljonne, G. Pourtois, C. Silva, E. Hennebicq, L. M. Herz, R. H. Friend, G. D. Scholes, S. Setayesh, K. Mullen, J. L. Bredas, *Proc. Natl. Acad. Sci. USA* **2002**, *99*, 10982–10987.

Received: February 25, 2008

Revised: May 4, 2008

Published online on June 18, 2008